COMPUTERS & SECURITY 55 (2015) 130–141

Available online at www.sciencedirect.com

ScienceDirect

journal homepage: www.elsevier.com/locate/cose

Computers & Security

Detecting seam carving based image resizing using local binary patterns

Ting Yin [a], *Gaobo Yang* [a,*], *Leida Li* [b], *Dengyong Zhang* [a], *Xingming Sun* [c]

[a] *School of Information Science and Engineering, Hunan University, Changsha, 410082, China*
[b] *School of Information and Electrical Engineering, China University of Mining and Technology, Xuzhou 221116, China*
[c] *School of Computer and Software, Nanjing University of Information Science & Technology, Nanjing 210044, China*

ARTICLE INFO

Article history:
Received 11 March 2015
Received in revised form 10 August 2015
Accepted 6 September 2015
Available online 11 September 2015

Keywords:
Content-aware image retargeting
Object removal
Seam carving
Local binary patterns
Blind forensic

ABSTRACT

Seam carving is the most popular content-aware image retargeting technique. However, it can also be deliberately used for object removal tampering. In this paper, a blind image forensics approach is proposed for seam-carved forgery detection. Since seam carving changes the local texture in an image, a local texture descriptor, i.e., local binary pattern (LBP), is exploited as pre-processing to highlight the local texture artifacts. Moreover, six new half-seam features are defined to unveil the energy changes in half images. They are combined with the existing eighteen energy bias and noise-based features to form twenty-four features. These features are extracted in LBP domain, instead of the conventional pixel-domain to highlight the local texture changes. Finally, support vector machine (SVM) classifier is exploited to determine whether an image is original or suffered from seam carving. Experimental results show that compared with the state-of-the-art methods, the proposed approach improves the detection accuracy by 3.5–19.1% for resized images with different scaling ratios.

1. Introduction

Content-aware image resizing (CAIR) has attracted increasing research attention with the rapid growth in mobile computing (Rubinstein et al., 2010). Among those CAIR techniques, seam carving (Avidan and Shamir, 2007) is the most widely accepted. Seam is defined as an eight-connected path of pixels, either vertically or horizontally. Successive removal of the optimal seams with lower energies allows reduction in image size. Because of its excellent performance, seam carving has been integrated into popular image processing softwares for adaptive scaling, such as Adobe Photoshop, GIMP, ImageMagic and iResizer. However, seam carving can also be deliberately used to remove an object from an image. Since the removed object is generally a semantic object, it might change the semantic content that an image conveys. Thus, seam carving can be deliberately used for object removal to achieve malicious purpose. Therefore, it is important to design a detection method for those images which suffer from the possible seam carving.

Up to present, there are a few existing approaches for the detection of seam carving operation. Lu et al. proposed an active forensics method based on forensic hash, which is actually the

* *Corresponding author*. Tel.: +(86)0731 8882 3141.
E-mail address: yanggaobo@hnu.edu.cn (G. Yang).
http://dx.doi.org/10.1016/j.cose.2015.09.003

side information specifically designed for image seam carving (Lu and Wu, 2011). However, it has two drawbacks: First, falsifiers can easily remove the forensic hash since it is attached at the header of an image file. Second, since forensics hash is an active method, it must be built in advance. The earliest work for the passive detection of image seam carving is proposed by Sarkar et al. (2009). Inspired by the statistical features for image steganalysis, 324-dimensional Markov features are exploited for seam carving detection. However, it only achieves a detection accuracy of no more than 77.3%. Fillion et al. proposed a set of image features such as wavelet absolute moments for the detection of seam carving (Fillion and Sharma, 2010), which achieves a detection accuracy up to 84.0% and 91.3% for resized images with scaling ratio of 20% and 30%, respectively. Later, some passive forensics approaches are proposed for the detection of seam carving in JPEG images. Liu et al. proposed a shift-recompression-based feature mining approach to detecting seam-carved forgery in JPEG images (Liu et al., 2012). It can discriminate forged JPEG images from intact JPEG images. Liu and Chen also addressed the seam-carved forgery detection from the steganalysis point of view (Liu and Chen, 2014). An improved detection approach is proposed for seam-carved forgery detection in JPEG images, which merges calibrated neighboring joint density and rich model-based steganalysis (Xia et al., 2014). Moreover, Chang et al. proposed another detection method to detect seam carving in JPEG images (Chang et al., 2013). It is based on the facts that the seam-carved forgery might destroy the regular symmetrical property of blocking artifact characteristics matrix (BACM). Eighteen features are defined to detect the damage of BACM, and the support vector machine (SVM) classifier is trained to determine whether an image is an original or it has been suffered from seam-carving. Recently, Wei et al. (2014) proposed a patch analysis method to detect seam carved images. Images are firstly divided into 2×2 blocks, referred to as mini-squares, and then searched for one of nine types of patches that are likely to recover a mini-square from seam carving. The patch transition probability among three-connected mini-squares is exploited to improve the detection accuracy. It is reported that accuracies of 92.2% and 95.8% are achieved for 20% and 50% seam-carved images, respectively. In addition, Ryu and Lee (2014) exploited the energy bias and noise of suspicious images to reliably unveil the traces of seam carving, and superior performance was achieved as well.

However, the existing approaches cannot fully meet the needs of forensics. We believe that if the inherent nature and important properties of the seam carving process are fully considered, there is still some scope to further improve the detection accuracy. Different from other image tampering techniques such as image-inpainting, removing seams from an image does not necessarily bring visually annoying artifacts such as ghosting shadow or blurriness. This is actually the main challenge for the blind detection of image seam carving. In most cases, removing seams from an image only changes the local texture and the energy distribution. Therefore, the key issue of detecting seam carving is to design more sensitive features which can reflect the inherent nature of the seam carving process.

In this paper, a novel blind detection approach is proposed for detecting image seam carving using local binary patterns (LBP). In essence, LBP is a local texture descriptor which has been widely used in various image analysis applications (Ojala et al., 1996, 2002). By experiments, we find that when seams are carved out from an image, there are significant changes for the LBP values of those pixels along a seam. Therefore, we are motivated to extract the statistical features in the LBP domain, since they will be more sensitive than the same features extracted from the conventional pixel-domain. Meanwhile, it is widely-known that image seam carving functions well by removing those seams with minimum cumulative energies defined by the energy function. After removing those seams with relatively lower energies, the energy distribution will be greatly changed. Thus, the design of forensics features for image seam carving should be closely related to the energy bias within an image. Furthermore, six new half-seam features are defined to unveil the energy bias in upper half images. These six features are combined with the existing eighteen energy bias and noise-based features (Ryu and Lee, 2014), but they are also extracted in the LBP domain to form twenty-four features for pattern classification. Specifically, support vector machine (SVM) classifier is exploited to determine whether an image is original or suffered from seam carving. Experimental results show that the proposed approach achieves superior detection performance over existing approaches.

The remainder of this paper is organized as follows. Section 2 briefly reviews seam carving algorithm. Improved energy feature work on LBP matrix is calculated in Section 3. The experimental results are reported in Section 4 and we conclude this paper in Section 5.

2. Image seam carving

CAIR indicates that visually important region of interest (ROI) is not affected (or minimally affected) by an image resizing process. Rubinstein et al. (2010) firstly introduced the concept of seam carving into CAIR techniques. By defining a gradient related energy function, the seams with lowest energy are identified (Dong et al., 2009; Rubinstein et al., 2008, 2010). A seam is an 8-connected path of pixels crossing the image from top to bottom, or from left to right. Therefore, a vertical seam for an $n \times m$ image I is defined as Eq. (1), where i and col(i) denote row coordinates and the corresponding column coordinates, respectively. A horizontal seam is also defined similarly.

$$\mathbf{s}^{\mathbf{v}} = \{I, col(i)\}_{i=1}^{n}, \text{ s.t. } \forall i, |col(i) - col(i-1)| \le 1 \tag{1}$$

By successively removing seams which have as low energies as possible, the important image content is preserved during the resizing process. For this reason, the energy of each pixel is first measured by the energy function e.

$$e(I) = \left|\frac{\partial}{\partial x} I\right| + \left|\frac{\partial}{\partial y} I\right| \tag{2}$$

From the energy function e at a pixel, the energy of a vertical seam $E(s)$ is defined as follows:

(a) an original image (b) the original image with vertical seams (c) the image after seam carving

Fig. 1 – Content-aware image resizing by seam carving.

$$E(s) = \sum_{i=1}^{n} e(i, col(i)), \text{s.t. } \forall i, |col(i) - col(i-1)| \leq 1 \quad (3)$$

Then, a vertical seam with the lowest energy path $s^* = minE(s)$ is found by dynamic programming with the recurrence relation M:

$$M(i, j) = e(i, j) + \min(M(i-1, j-1), M(i-1, j), M(i-1, j+1)) \quad (4)$$

After constructing a cumulative minimum energy matrix M for all possible seams, the lowest energy seam s^* is found by back-tracking from the minimum value of the last row in M. By iteratively eliminating the selected seam, which has lowest energy, the size of a given image is reduced without destroying salient image contents. Please note that removing a seam from an image only has limited local effects, though all the rest of pixels at the right side of this seam are shifted left to compensate the missing path. That is, the possible visual artifacts merely occur near the removed seam, leaving the rest of the image intact. Fig. 1 is an example of CAIR by seam carving, where the vertical seams to be removed are marked in red. By removing the vertical seams, the image width is decreased up to 30%. As shown in Fig. 1(c), the most important content still remains steady without visually noticeable artifacts.

In general, image retargeting usually leads to three kinds of distortions including global structure deformation, local texture deformation and information loss (Hsu et al., 2014). When an image is over-squeezed in the process of seam carving, there usually exists global structural distortion, which is quite visually unpleasant shape deformation of prominent objects. This implies that users can easily perceive the global structure distortion without the aid of passive forensics. For the information loss, it is an ill-posed problem itself. In Hsu et al. (2014), the saliency loss ratio (SLR), which is defined as the ratio of the sums of saliency values for the images after and before retargeting, is used to measure the information loss. Since the computation of SLR requires the saliency map of the original image, the information loss is not a suitable clue for the blind detection of image seam carving. Moreover, the content information loss alone does not have significant impacts on the final perceptual quality of the retargeted image.

From the above analysis, it is not difficult to know that the local texture distortion is the most important clue for the forensics of image seam carving. Specifically, the reasons are two-fold. First, the local texture deformation is not as much visually unpleasant as the global structure distortion, which brings greater challenge for passive forensics. Second, only when there is no global geometric/structure distortion in the retargeted image, it makes sense to image seam carving for users. Actually, the main idea behind this paper is to highlight the local texture distortion so as to design robust feature for passive forensics.

3. Proposed blind forensics approach

As claimed in the precious section, the local texture distortion is a crucial clue for the blind forensics of image seam carving. Meanwhile, because image seam carving is achieved by successively removing seams with low energies defined by an energy function, the energy features are also very important for the detection of seam carving. Therefore, we attempt to consider both the local texture and the global energy distribution in the design of statistical features for blind forensics. In this paper, the statistical features specifically designed for forensics can be divided into two pipelined parts. The first part probably reveals the artifacts in the local texture area, and the second part inspects the change of energy distribution when seams with relatively low energies are removed.

Fig. 2 is the general framework of the proposed approach. The suspicious image is firstly processed with LBP detector, and then 24 energy features are extracted from the LBP image to measure the energy bias of the suspicious image. The 24 energy features consist of 18 energy feature similar to Ryu and Lee (2014) and 6 new energy features were defined on the basis of half seam. Since these energy features are extracted from the LBP image, they can reflect the changes of both the local texture and the global energy distribution. Next, the feature vectors are applied to train and test support vector machine (SVM) classifier. Finally, a decision about whether an image suffered from seam-carving or not is determined. In the following subsections, we first explain the LBP detector to unveil the local texture artifacts. Then, the 24 energy features, especially the six new half-seam energy features, are discussed. Finally, the SVM classifier for blind forensics is briefly described.

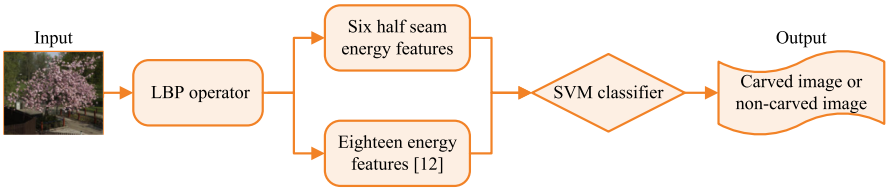

Fig. 2 – The proposed detection framework of seam carving forensics.

3.1. *LBP based image pre-processing*

Image seam carving does not introduce any new pixels in the image. Therefore, removing vertical or horizontal seams from an image does not necessarily lead to any common artifacts such as blurriness or ghosting shadow. When a vertical seam is removed, the intuitive change is that all those pixels at the right side are shifted left to compensate for the missing path. Thus, the artifacts for seam carving are mainly the change of local texture, especially near those regions with prominent edges. Although inter-pixel correlation and co-occurrence matrix have been used to represent this artifact, they are actually not effective to measure the kind of artifacts, especially the process of seam removal.

LBP is a local texture descriptor widely used in image analysis because of its superior performance. In this paper, LBP is exploited to measure the texture variation during image seam carving. Fig. 3 shows the basic LBP operator. Given a pixel in the image, an LBP code is computed by comparing it with its neighbors:

$$LBP_{P,R} = \sum_{p=0}^{P-1} s(g_p - g_c)2^p, \quad s(x) = \begin{cases} 1, & x \geq 0 \\ 0, & x < 0 \end{cases} \tag{5}$$

where g_c is the gray value of the central pixel, g_p is the value of its neighbors, P is the total number of involved neighbors, and R is the radius of neighborhood. In this example, R equals 1, and P will be 8, which means the 8-connected neighboring pixels are involved in the LBP computation. Then, it is encoded into an 8-bit integer value. Thus, the input image is transformed into another LBP image by recursive computation of the LBP value of each pixel.

When a vertical seam is removed, all the pixels on its right side are shifted left to fill the gap of the removed path. For those pixels exactly adjacent to this seam, their 8-connected neighboring pixels will be significantly changed. Thus, their LBP codes will be quite different from their original ones. Fig. 4 shows such an example of the LBP changes when a seam is removed. For simplicity, a 5*7 block in the original image is enlarged to illustrate the influence of removing a seam toward the LBPs of those pixels adjacent to this seam. In Fig. 4, the upper row shows the pixel values of the original block and their LBPs. Those pixels which form the seam to be removed are marked in blue. The LBP values of those pixels in the interior 3*5 block are also shown. By removing this seam, the 5*7 block turns into a 5*6 block because one pixel is removed each row. It is apparent that those pixels marked in yellows which are not horizontally adjacent are 8-connected pixels this time. The LBP values of its interior 3*4 block are shown as well. By observation, we can conclude that when a seam is removed from an image, there are significant changes for the LBP values of those neighboring pixels along the seam. That is, LBP is sensitive to the texture change of carved image, especially those pixels along the removed seam. This implies that LBP is beneficial to describe statistical changes caused by image seam carving.

In the following, we further analyze the influence of seam-carving toward the LBP values of those neighboring pixels along the seam, which is shown in Fig. 5. The original image, one vertical seam and the image after removing a seam are shown in Fig. 5(a), (b) and (c), respectively. For each pixel in the vertical seam, there are two pixels at the left and right sides, respectively. That is, there are two columns of pixels which are closely adjacent to the seam. Fig. 5(d) and (e) shows the difference of the LBP values in part for those two columns of pixels at the left and right sides between original image and seam carved image, respectively. It is apparent that there are significant changes for the LBP values of these two columns after a seam is removed from an image. Thus, we can conclude that when a seam is removed from an image, there are significant changes for the LBP values of those neighboring pixels along the seam. That is, LBP is sensitive to the texture change of carved image, especially those pixels along the removed seam. The inherent reason behind this is that a linear weighting mechanism is involved in the generation of LBP code. When a seam is removed, not only their neighboring pixels are changes for those pixels along the seam, but also the weighting

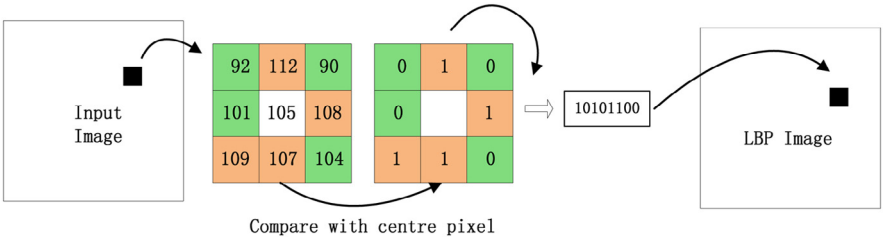

Fig. 3 – The basic LBP operator.

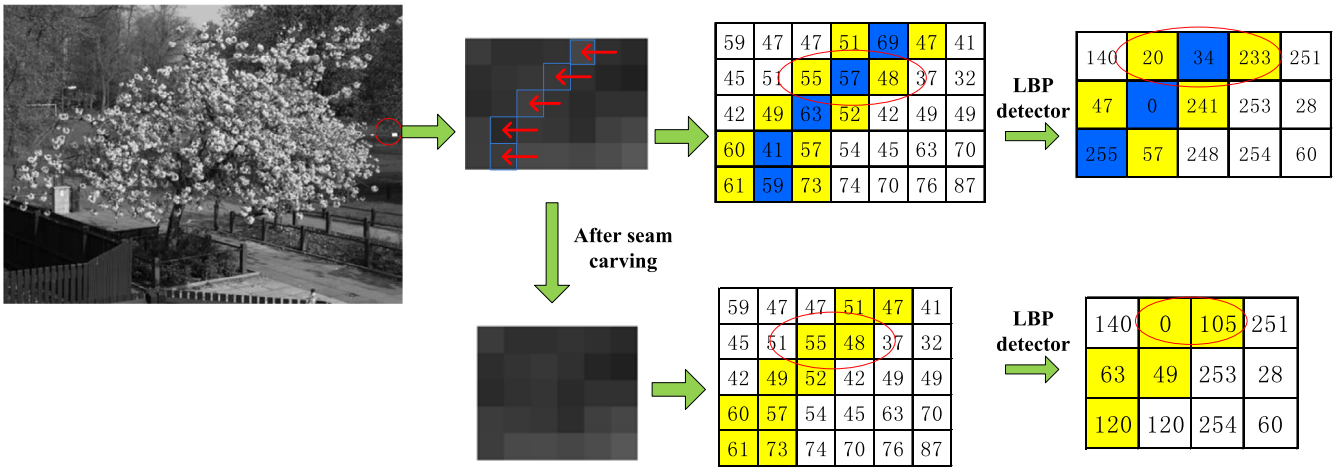

Fig. 4 – Examples of LBP influence for removing a pixel. (For interpretation of the references to color in this figure legend, the reader is referred to the web version of this article.)

mechanism highlights the change of local texture. Therefore, the introduction of LBP is beneficial to the description of statistical texture changes caused by image seam carving.

3.2. *Energy features in LBP domain*

As claimed in the previous section, the statistical feature for seam carving forensics should be closely related to the energy bias. The direct influences of seam carving to the energy distribution of image are two-fold. First, the energy distribution of seam carved images is relatively higher than that of non-carved images since the seams with low energies are removed. Second, the energy distribution of the seam-carved image should be relatively smoother than that of the original image. In this paper, the statistical features are also defined following the idea of energy bias. Specifically, the energy features in Ryu and Lee (2014) are still kept for forensics, but they are measured in LBP domain, instead of the intensity image in pixel domain.

In the following, the 18 statistical features in Ryu and Lee (2014) are briefly introduced. They can be classified into three categories: energy-based, seam-based and noise-based. The energy-based features include the average energy, the average column energy, the average row energy and the average energy difference. For the seam-based features, they are computed for both row and column directions. After constructing a cumulative minimum energy matrix M for all possible seams, five statistics values called min, max, mean, standard deviation and the difference between maximum and minimum values are computed for both the column and row directions, respectively. Thus, the number of seam-based energy features is 10. The idea behind noise-based statistical features is that the seam carving process affects the noise level of the retargeted images as well, simply because it generally removes those flat regions. Let I be the candidate image to be detected and F be the Winner filter with 5×5 window. The noise is extracted by subtracting the filtered image from the original one. That is, the noise of a given image $N(i, j)$ is computed by $N = I - F(I)$. Finally, the mean, standard deviation, skewness and kurtosis of the noise are computed as the statistical features for forensics. For more detailed information about these features, refer to Ryu and Lee (2014).

Moreover, six new energy features are proposed to enrich the statistical features and improve the forensics accuracy. They are defined on the basis of half-seam, instead of the whole seam. The motivation behind this are illustrated in Fig. 6, where a blue line traces the lowest energy path through 50% of the image and the red line traces lowest energy path through the whole image. From the figure, we observe that the lowest energy path of an image is not the lowest energy for half of an image. Therefore, for the upper part of a carved image, the removed seams in the whole image are not the optimal seam. It means that the local artifacts may be more obvious in the upper part of a carved image. Thus, we proposed half-seam energy to measure the local artifacts of image. Similar to the seam-based features, the half-seam-based features are computed upon a cumulative minimum energy matrix M on half of image, then three statistics values called min, max and mean are computed at specified column and row, respectively. Table 1 summarizes the six half-seam features. Totally, we obtain $18 + 6 = 24$ LBP-based energy features.

3.3. *SVM classifier for passive forensics*

After extracting the twenty-four statistical features, a pattern recognition classifier is required to determine whether the image under investigation is seam-carved or not. In this paper, support vector machine (SVM) is adopted as the classifier, simply because it is a supervised learning method commonly used for classification. In the training phase, two classes of images (seam-carved or not-carved) are represented by the above feature vectors. Then, the classifier attempts to find an optimal linear decision surface called the maximum margin hyper plane by maximizing the geometric margin between the closest instances on either side. To further improve the classification accuracy, the feature vectors are non-linearly projected into a high dimensional feature space by Radial Basis Function (RBF) kernel. In the final classification stage, a feature vector extracted from the image under investigation is input into the classifier after training. Therefore, the image under investigation will be classified into either class of image: seam-carved or non-carved.

(a) the original image (b) the original image with a vertical seam (c) the image after removing a seam

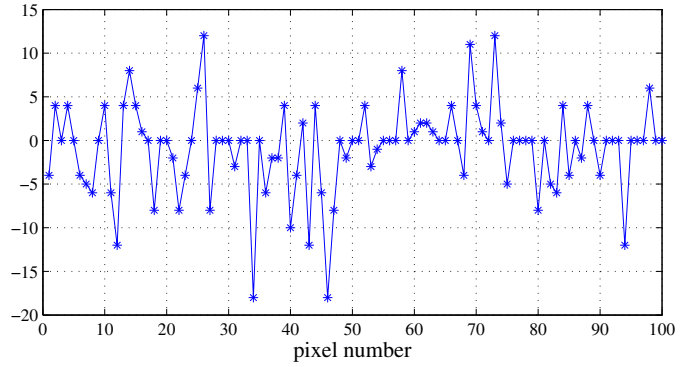

(d) the difference of the LBP values for those pixels at the left side of removed seam between the original image and the seam-carved image

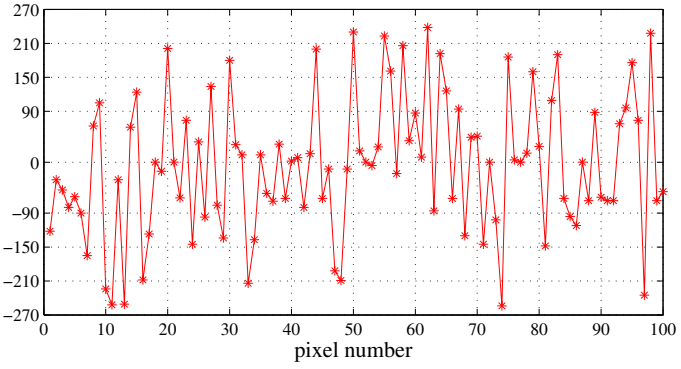

(e) the difference of the LBP values for those pixels at the right side of removed seam between the original image and the seam-carved image

Fig. 5 – The LBP changes of removing a seam.

Table 1 – Six new features based on cumulative minimum energy matrix M.

Feature	Description	Feature	Description
Half-vertical seam_{max}	$\max_{j=1}^{n} M\left(\frac{m}{2}, j\right)$	Half-horizontal seam_{max}	$\max_{i=1}^{m} M\left(i, \frac{n}{2}\right)$
Half-vertical seam_{min}	$\min_{j=1}^{n} M\left(\frac{m}{2}, j\right)$	Half-horizontal seam_{min}	$\min_{i=1}^{m} M\left(i, \frac{n}{2}\right)$
Half-vertical seam_{mean}	$\frac{1}{n}\sum_{j=1}^{n} M\left(\frac{m}{2}, j\right)$	Half-horizontal seam_{mean}	$\frac{1}{m}\sum_{i=1}^{m} M\left(i, \frac{n}{2}\right)$

Fig. 6 – Optimal seam path through 50% and 100% of an image. (For interpretation of the references to color in this figure legend, the reader is referred to the web version of this article.)

4. Experimental results and analysis

4.1. *Experimental environment setup*

In this section, the experimental results of an extensive series of blind detection are reported to evaluate the performance of the proposed approach. The hardware configuration of experiments is a personal computer (Intel® Core(TM) i5-2450M CPU @ 2.5 GHz, 4.0 GB RAM), and the forensics detector is implemented with MATLAB 7.0. The SVM classifier is directly downloaded from LibSVM (Chang and Lin, 2000), and Radial Basis Function (RBF) is used as the kernel. Optimal kernel parameters are found via grid search and 3-fold cross validation strategy. Moreover, Python and Gnuplot are used for the parameter optimization of SVM.

To the best of our knowledge, there is no public-available image database for the performance evaluation of seam carving forensics. Thus, we build a test image library for seam carving detection by ourselves. Firstly, the UCID image database (Schaefer and Stich, 2004), which is widely used for image quality assessment, is chosen as the benchmark because of its rich content varieties. It is made up of 1338 color images with the same spatial resolution (384×512 pixels/image). These images have quite different contents including human, landscape, buildings, animals, and so on. Secondly, to evaluate the robustness and sensitivity of our method, several experiments are conducted in the following scenarios: (1) images with large scaling ratios; (2) images with small scaling ratios and (3) images with mixed scaling ratios. Thus, three test image libraries are built for the above-mentioned three scenarios. In the first case, 1338 untouched images are resized by seam carving (Rubinstein et al., 2010), and the scaling ratios vary from 10% to 50% with a step size of 10%. That is, the scaling ratios are 10%, 20%, 30%, 40% and 50%, respectively. As a result, there are 6690 tampered images, which are mixed with the 1338 original images for our experiments. In the second case, the scaling ratios vary from 3% to 21% in a step size of 3%. Thus, there are 9366 tampered images for the experiments of images with small scaling ratios. In the third case, the tampered images used in the above two scenarios are mixed together to form a new test library. Please note that the 9% and 21% in small scaling ratios are very near to 10% and 20% in large scaling ratios, respectively. To avoid too many images with similar scaling ratios, those images with the scaling ratios of 10% and 20% are removed from the new test library. As a consequence, 1338 original images, 9366 small scaling ratios tampered images, and 4014 large scaling ratio tampered images are used in the third case. Finally, these images are divided into several groups to evaluate the performance of our proposed approach under different cases. To make comparisons with the existing approaches, two most state-of-the-art works (Wei et al., 2014; Ryu and Lee, 2014) are chosen as the ground-truth. That is, there are three detectors for experiments, which are tested with the same hardware environment and test image libraries.

4.2. *Experimental results for carved images with different scaling ratios*

We test the detection performance of image seam carving with the same scaling ratio. For each scaling ratio, there are 1338 original images and 1338 resized images. To ensure the randomness of our experiments, 4-fold cross validation strategy is exploited. That is, the 24 features are recorded over a random training set of 2006 images, and the performance is measured on the remaining 670 images. It is repeated five times, and the average performance measures are recorded.

4.2.1. *Images with large scaling ratios*

Table 2 summarizes the comparison results of detection accuracy among the three detectors. It is apparent that with the increase of scaling ratio, the detection accuracies of these three detectors increase as well. On average, the proposed approach achieves the best detection accuracy, which is about 12.95% and 11.70% higher than that of Wei et al. (2014) and Ryu and Lee (2014), respectively. For the patch-based detector (Wei et al., 2014), it only considers the optimal type of patches for each mini-square and does not explicitly take into account the changes of local texture and energy due to image seam carving. Thus, its performance is the worst, especially for those resized images with relatively small carving ratio. Ryu and Lee (2014) exploit the energy bias and noise level of suspicious image to unveil the traces of seam carving. It is more closely related to the inherent nature of seam carving, which leads to much better

Table 2 – Comparison of detection accuracy for carved images with large scaling ratios.

Scaling ratios	Accuracy (%)		
	Patch-based detector (Wei et al., 2014)	Energy-based detector (Ryu and Lee, 2014)	Proposed approach
10%	57.91	65.22	80
20%	74.18	75.37	94.48
30%	91.34	85.52	98.66
40%	89.70	91.94	99.85
50%	94.93	96.27	99.85

detection accuracy compared with the patch-based detector. Our proposed approach is actually an improvement to the energy-based method (Ryu and Lee, 2014). The detection accuracy improves by the minimum of 3.58% to the maximum of 19.11% for scaling ratios of 50% and 20%, respectively. For the seam carving with the scaling ratio of only 10%, which is the most difficult to detect, our proposed approach achieves an accuracy of 80%. Even though it is not high enough, it is still acceptable for practical use because it is unlikely to remove an object from an image for malicious forgery with a scaling ratio of only 10%. Actually, the significant improvement of detection performance mainly benefits from the fact that the statistical features in LBP domain is more sensitive to the change of local texture than those extracted in pixel domain. That is, it unveils the local texture artifacts due to image seam carving much better.

Moreover, the performance of the proposed approach is further tested under the case of mixed image set with large scaling ratios. In the actual forensics practice, the scaling ratio of seam carving is unknown to the forensics analyst. Thus, 268 images are randomly selected from the resized images by seam caving with each scaling ratio. In sum, there are 1340 resized images. They are missed with the 1338 original images to build a mixed set with 2678 images for training. The rest 5350 resized images are used as the image test set for performance evaluation. The experimental results are reported in Table 3. It is apparent that the proposed approach achieves the best detection performance.

4.2.2. *Images with small scaling ratios*

In this experiment, the effectiveness of the proposed method is shown for those images with small scaling ratios from 3% to 21%. Table 4 compares the detection accuracies among the three detectors. It is apparent that our method also achieves the highest detection accuracy, which is about 17.73% and 13.45% higher on average than that of Wei et al. (2014) and Ryu and Lee (2014), respectively. Of course, the detection accuracies of small scaling ratios are less than those of large scaling ratios, which is straightforward to understand. Moreover, for images with small scaling ratios, the proposed approach has more advantages. Specifically, when the scaling ratio is 12%, the proposed approach achieves the same performance of the state-of-the-art methods when the scaling ratio are 15% or more. The performance of mixed image set with small scaling ratios is also tested, and the experimental results are reported in Table 5. Compared with the state-of-the-art methods, the proposed approach achieves the best performance except for the scaling ratios of 3% and 6%, which are not often for image seam carving with such a low scaling ratio. Therefore, it can be concluded that the proposed approach outperforms the state-of-the-art methods on a whole.

Table 3 – Detection accuracy of the proposed detector for mixed sets with large scaling ratios.

Scaling ratios	Accuracy (%)		
	Patch-based detector (Wei et al., 2014)	Energy-based detector (Ryu and Lee, 2014)	Proposed approach
10%	24.67	32.80	51.78
20%	61.59	61.68	93.55
30%	89.35	83.46	99.35
40%	91.03	95.23	99.81
50%	95.89	98.78	100
Average	72.50	74.39	88.90

Table 4 – Comparison of detection accuracy for carved images with small scaling ratios.

Scaling ratios	Accuracy (%)		
	Patch-based detector (Wei et al., 2014)	Energy-based detector (Ryu and Lee, 2014)	Proposed approach
3%	50.22	54.48	55.53
6%	53.59	57.88	65.17
9%	56.99	60.99	74.55
12%	58.21	64.13	81.20
15%	63.13	70.59	90.17
18%	71.94	73.84	92.04
21%	74.78	76.91	94.32

Table 5 – Detection accuracy of the proposed detector for mixed sets with small scaling ratios.

Scaling ratios	Accuracy (%)		
	Patch-based detector (Wei et al., 2014)	Energy-based detector (Ryu and Lee, 2014)	Proposed approach
3%	22.32	34.18	29.29
6%	27.24	40.89	39.32
9%	34.14	45.16	51.77
12%	38.54	50.48	62.16
15%	47.59	58.06	87.01
18%	52.91	61.90	93.11
21%	56.64	67.31	97.21
Average	39.91	51.14	65.70

4.2.3. *Images with mixed scaling ratios*

In order to demonstrate the universality and robustness of the proposed approach, those resized images with large and small scaling ratios are mixed together for performance evaluation. The ROC curves for the three detectors are shown in Fig. 7, in which each sub-figure represents the ROC performance under different scaling ratios from 6% to 50%, respectively. The probabilities of true positive (TP) and false positive (FP) are determined with a threshold (ranges from 0 to 1), which is calculated by the percent of correctly classified carved images and the percent of incorrectly classified non-carved images, respectively. Compared with the patch-based method (Wei et al., 2014), the proposed approach increases the true positive rate (TPR) by at least 18% on average with lower false positive rate (<0.05). Moreover, due to the introduction of LBP pre-processing into feature extraction, the true positive rate increases at least 15% than the energy-based method (Ryu and Lee, 2014). Even when a very low probability of false positive rate (FPR) is enforced to 1% (except for the case of the scaling ratios below 10%), the proposed approach still remains a high probability of correct detection up to 90%. This also confirms the robustness of the LBP-based energy features.

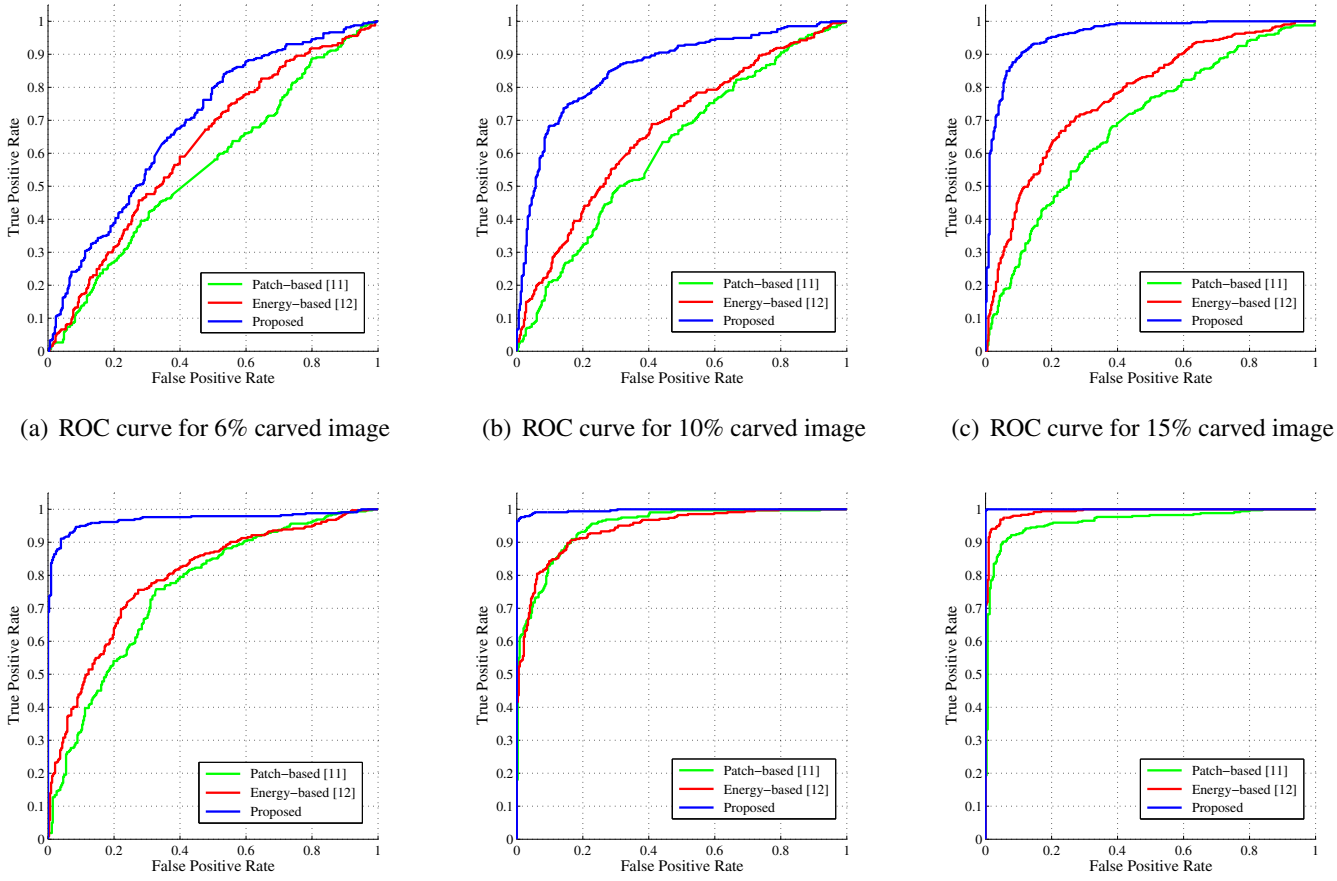

(a) ROC curve for 6% carved image (b) ROC curve for 10% carved image (c) ROC curve for 15% carved image

(d) ROC curve for 20% carved image (e) ROC curve for 30% carved image (f) ROC curve for 50% carved image

Fig. 7 – Comparison of ROC curves among the proposed method and two existing detectors.

4.3. *Experimental results under different mixing ratios between the training set and the test set*

The proposed approach is also tested with different sample proportions for the SVM classifier. The experimental results are shown in Table 6. Under five different mixing ratios between the training set and the test set, the proposed approach achieves the best detection accuracies. Though the proposed approach achieves the best performance when the mixing ratio is 3:1, there is only minor difference of detection accuracies under different mixing ratios. Thus, the proposed approach is not sensitive to the mixing ratio between the training set and the test ratios.

Moreover, similar to Ryu and Lee (2014), we also test the discrimination capability of every type of feature vectors. The experimental results are reported in Table 7. It is worth to notice that the newly proposed statistical features defined on the basis of half-seam do benefit to the improvement of detection accuracy, and reveal best performance among the proposed features. However, the introduction of LBP pre-processing into the feature extraction plays a key role in the improvement of detection accuracy.

Table 6 – Detection accuracy of the proposed detector under different mixing ratios between the training samples and the test

Scaling ratios	Training set:Test set				
	3:1	2:1	1:1	1:2	1:3
3%	**55.53**	53.76	54.56	51.91	54.56
6%	**65.17**	63.85	63.83	63.79	64.87
9%	**74.55**	74.16	72.05	72.98	71.38
12%	**81.20**	80.55	79.60	79.93	78.77
15%	**90.17**	89.52	89.31	87.44	88.64
18%	**92.04**	92.04	91.55	91.70	91.63
21%	**94.32**	93.95	93.20	93.83	94.92
30%	**98.66**	98.43	98.21	97.76	97.41
40%	**99.85**	98.99	99.18	99.44	99.30
50%	**99.85**	99.89	99.93	99.66	99.70

Boldface means the highest detection accuracy in each row.

4.4. *Detection results of JPEG image by image seam carving*

Due to the fact that a vast amount of digital images is stored in JPEG format, the performance of the proposed method against JPEG image is tested in this section. Each original images is JPEG compressed with a quality factor QF from 75 to 95 in steps of 5. The tampered images are first decompressed, seam carving, and JPEG compressed with the same QF with the first quality factor. The detection results are reported in Table 8. The

Table 7 – Detection accuracy of the proposed method by four feature vectors; breakdown by feature vector and the amount of seam carving.

Scaling ratios	Intensity-based (%)					Proposed approach (%)				
	Energy	Noise	Seam	Half-seam	All	Energy	Noise	Seam	Half-seam	All
3%	50.82	50.93	53.85	51.53	54.04	50.04	52.35	52.39	51.64	55.53
6%	51.68	51.98	56.84	53.96	58.41	50.26	56.24	55.08	55.98	65.17
9%	52.69	53.03	58.86	55.49	61.58	50.82	60.31	60.31	62.22	74.55
12%	53.74	54.45	64.42	57.59	65.88	51.87	64.13	64.76	66.37	81.20
15%	55.57	56.84	64.42	60.80	72.31	53.10	70.14	72.27	74.10	90.17
18%	56.91	58.63	66.41	61.92	75.67	53.96	73.21	75.67	77.95	92.04
21%	58.18	60.35	68.35	63.42	78.81	54.37	76.46	79.41	80.75	94.32
30%	63.98	67.64	74.59	69.39	88.38	58.15	87.07	87.89	90.02	98.66
40%	70.33	73.58	80.34	76.05	94.96	62.48	93.16	93.91	95.14	99.85
50%	76.42	80.49	85.28	82.06	98.51	66.93	97.23	97.79	98.06	99.85

Table 8 – Comparison of detection accuracy of JPEG image by seam carving.

Quality factors	Accuracy (%)		
	Patch-based detector (Wei et al., 2014)	Energy-based detector (Ryu and Lee, 2014)	Proposed approach
75	71.52	75.45	91.11
80	71.94	75.37	91.85
85	72.68	76.05	92.49
90	73.13	76.72	92.38
95	73.88	77.17	93.57

proposed method generally yielded the best performance. It shows that not only the proposed method can detect the original images, but also the JPEG images.

4.5. *Detection results of seam-carved and original images at the same image size*

Seam carving is the most popular content-aware image retargeting technique. Actually, it can be used for both image shrinkage and image enlargement to change the spatial resolution of digital image. Thus, if image shrinkage and image enlargement are combined together, it is easy for the users to change the image content by seam carving. Moreover, the original image size can be retained simultaneously. Therefore, another blind detection experiments are conducted on those resized images by seam carving, which have the same sizes as the original image. Firstly, ten images are randomly chosen from the UCID image library as the original images, which are firstly carved with a scaling ratio of 20% and then enlarged to their original sizes by seam carving. Then, the three detectors are used to detect those images after image shrinkage and image enlargement. The experimental results are summarized in Table 9. It shows that the proposed approach achieves a detection accuracy of 85.5%, which is a little lower than that of the patch-based approach but significantly better than that of the energy-based approach. Moreover, the detection accuracy is a little lower than that of those images with simply 20% shrinkage.

Table 9 – Comparison of detection accuracy of seam-carved and original images at the same image size.

Quality factors	Accuracy (%)		
	Patch-based detector (Wei et al., 2014)	Energy-based detector (Ryu and Lee, 2014)	Proposed approach
75	88.50	51.50	85.50

4.6. *Detection results of object removal by image seam carving*

Beside the conventional image resizing, seam carving can also be used for object removal. Moreover, object removal is often forgery operation with malicious purpose, since it might change the semantic content that an image delivers. Thus, we also test the detection performance of object removal forgery via seam carving. Ten test images after object removal are tested with the proposed approach. Due to space restriction, only one example of removing the object from an image by seam carving is shown in Fig. 8. The object to be removed is firstly marked with a bounding box, as shown in Fig. 8(a). The seams passing through the object to be removed are shown in Fig. 8(b), and the final image after object removal is shown in Fig. 8(c). Apparently, there are no visually annoying artifacts after object removal. However, the experimental results show that the proposed approach can effectively made binary decision that nine images have been suffered from seam carving. That is, only one image is missed in the forensics detection. As shown in Fig. 8(a), the object to be removed usually occupies a relatively big region, and thus the scaling ratio of image seam carving is not small. In this example, the scaling ratio is 15.2% in the horizontal axis. The detection accuracy of object removal is actually similar to the results reported in Table 4.

4.7. *Discussion*

The previous experimental results show that the proposed approach which extracts energy features in LBP domain achieves superior detection performance over existing approaches. Compared with the pixel-domain features, the proposed approach noticeably improves the detection performance. Specifically, the proposed approach is not only effective to detect image

(a) original image with an object marked with a bounding box (b) the seams passing through the object to be removed (c) the final image after object removal

Fig. 8 – Example of object removal from an image by seam carving.

shrinkage by seam carving, but also effective for the detection of deliberate object removal and seam-carving forgery in JPEG images. The inherent reason is that since seam carving changes both the local texture and the global energy distribution, the energy features extracted in LBP domain not only unveil the energy changes in tampered images but also highlight the local texture artifacts. However, the patch-based detection approach outperforms the proposed approach when they are used to detect those seam-carved images with the same sizes with the original ones. The preliminary reasons are analyzed as follows. In a broad sense, any change to digital image can be regarded as a tampering operation. That is, those seam-carved images retaining the same spatial resolutions actually suffer from both image shrinkage and image enlargement. They can be treated as two separate tampering operations, and their artifacts might be mixed together to form the ambiguous processing artifacts. The patch-based detection approach utilizes the Markov feature based on patches for passive forensics, which is actually a universal feature for forensics. Any changes, especially the image shrinkage and enlargement, will change the patch structure. However, the proposed approach is mainly based on the energy change in LBP domain to detect the forgery operation. Especially, when seams are inserted to enlarge the image size, it will change the image energy distribution as well. This will counteract the change of energy distribution caused by image reduction, which leads to the degradation of detection performance.

5. Conclusions and future work

Seam carving is a popular CAIR technique to adapt the image display on different terminals. It achieves a trade-off between the protection of visually important regions and the maintenance of overall image content. That is, seam carving achieves image resizing in a manner without leaving any visually noticeable artifacts. Since image seam carving can be used as a tool for malicious object removal, it is desirable but challenging to detect this kind of forgery operation. In this paper, a LBP-based improved feature mining approach is proposed to the blind forensics of image seam carving. Extensive experimental results show that the proposed approach achieves better detection accuracy compared with the existing approaches. However, the detection result is only a binary decision about whether an image has been seam carved or not. For future research, we will investigate the location of tampered regions (Li et al., 2015). Specifically, since geometric distortion is another main artifact of image seam carving, more robust statistical features should be investigated to reveal the change of geometric distortion, especially when semantic object is removed by seam carving.

Acknowledgements

This work is supported in part by the National Natural Science Foundation of China (61379143, 61232016, U1405254), the program for New Century Excellent Talents in University (NCET-11-0134), the Specialized Research Fund for the Doctoral Program of Higher Education (SRFDP) under grant 20120161110014 and the S&T Program of Xuzhou City (XM13B119) and the PAPD fund. We also appreciate the nice help from Mr Moses Odero for his improving the English usages in this paper.

Appendix. Supplementary material

Supplementary data to this article can be found online at doi:10.1016/j.cose.2015.09.003.

REFERENCES

Avidan S, Shamir A. Seam carving for content-aware image resizing. ACM Trans Graph 2007;26(3):10–16.

Chang WL, Shih TK, Hsu HH. Detection of seam carving in JPEG images. In: Awareness science and technology and ubi-media computing, international joint conference on IEEE. 2013. p. 632–8.

Dong W, Zhou N, Paul JC. Optimized image resizing using seam carving and scaling. ACM Trans Graph (TOG) 2009;28(5):112–25.

Fillion C, Sharma G. Detecting content adaptive scaling of images for forensic applications. IS&T/SPIE Electronic Imaging, International Society for Optics and Photonics, p. 75410Z, 2010.

Hsu C, Lin C, Fang Y, Lin W. Objective quality assessment for image retargeting based on perceptual geometric distortion and information loss. IEEE J Select Top Signal Process 2014;8(3):377–89.
Li J, Li X, Yang B, Sun X. Segmentation-based image copy-move forgery detection scheme. IEEE Trans Inform Forensics Secur 2015;10(3):507–18.
Chang C, Lin C. LibSVM: a library for support vector machines. <http://www.csie.ntu.edu.tw/~cjlin/libsvm/> 2000.
Liu Q, Chen Z. Improved approaches with calibrated neighboring joint density to steganalysis and seam-carved forgery detection in JPEG images. ACM Trans Intell Syst Technol (TIST) 2014;5(4):63.
Liu Q, Li X, et al. Shift recompression-based feature mining for detecting content-aware scaled forgery in JPEG images. Proceedings of the twelfth international workshop on multimedia data mining, pp. 10–16, 2012.
Lu W, Wu M. Seam carving estimation using forensic hash. Proceedings of the thirteenth ACM multimedia workshop on multimedia and security, pp. 9–14, 2011.
Ojala T, Pietikainen M, Harwood D. A comparative study of texture measures with classification based on featured distributions. Pattern Recognit 1996;29(1):51–9.
Ojala T, Pietikainen M, Maenpaa T. Multiresolution gray-scale and rotation invariant texture classification with local binary patterns. IEEE Trans Pattern Anal Mach Intell 2002;24(7):971–87.
Rubinstein M, Shamir A, Avidan S. Improved seam carving for video retargeting. ACM Trans Graph (TOG) 2008;27(3):1–16.
Rubinstein M, Sorkine O, Shamir A. A comparative study of image retargeting. ACM Trans Graph (TOG) 2010;29(6):151–60.
Rubinstein M, Gutierrez D, Sorkine O, et al. A comparative study of image retargeting. ACM Trans Graph (TOG) 2010;29(6):160–70.
Ryu SJ, Lee HY. Detecting trace of seam carving for forensic analysis. IEICE Trans Inform Syst 2014;97(5):1304–11.
Sarkar A, Nataraj L, Manjunath BS. Detection of seam carving and localization of seam insertions in digital images. Proceedings of the 11th ACM workshop on multimedia and security, pp. 107–16, 2009.
Schaefer G, Stich M. UCID – An Uncompressed color image database. In: Proc. of SPIE, storage and retrieval methods and applications for multimedia, 5307. 2004. p. 472–80.
Wei JD, Lin YJ, Wu YJ. A patch analysis method to detect seam carved images. Pattern Recognit Lett 2014;36:100–6.
Xia Z, Wang X, Sun X, Wang B. Steganalysis of least significant bit matching using multi-order differences. Secur Commun Networks 2014;7(8):1283–91.

Ying Ting is a master student in the School of Information Science and Engineering, Hunan University, China. Her research interests are in the area of image passive forensics for content-aware image and video retargeting.

Gaobo Yang is a full professor in the School of Information Science and Engineering, Hunan University, China. He is also a member of Hunan Provincial Key Lab of Networks and Information Security. During August 2010 to July 2011, he made an academic visit to the University of Surrey, UK. His research interests are video information security.

Leida Li is an associate professor in the School of Information and Electrical Engineering, China University of Mining and Technology. He obtained his PhD degree from Xidian University, China in 2010. During January 2014 to January 2015, he made his academic visit to Nanyang University of Technology, Singapore. His research interests include image quality assessment and image forensics.

Dengyong Zhang is a PhD student in the School of Information Science and Engineering, Hunan University, China. His research interests are in the area of passive forensics for image and video forgery.